Robotica (2017) volume 35, pp. 1541–1561. © Cambridge University Press 2016
doi:10.1017/S0263574716000308

# Increase the feasible step region of biped robots through active vertical flexion and extension motions

Wei Gao†, Zhenzhong Jia‡ and Chenglong Fu§¶*

†*School of Aerospace, Tsinghua University, Beijing, 100084, P. R. China.*
*E-mail: gaow13@mails.tsinghua.edu.cn*
‡*The Robotics Institute, Carnegie Mellon University, Pittsburgh, PA, 15213, USA.*
*E-mail: zhenzjia@cmu.edu*
§*State Key Laboratory of Tribology, Tsinghua University, Beijing, 100084, P. R. China*
¶*Beijing Key Laboratory of Precision/Ultra-precision Manufacturing Equipments and Control, Tsinghua University, Beijing, 100084, P. R. China*

(Accepted April 18, 2016. First published online: May 20, 2016)

**SUMMARY**
This paper investigates the active vertical motion of biped systems and its significance to the balance of biped robots, which have been commonly neglected by the use of a well-known model called the Linear Inverted Pendulum Model. The feasible step location is theoretically estimated by considering the active vertical movement on a simple point mass model. Based on the estimation, we present two new strategies, namely the flexion strategy and the extension strategy, to enable biped robots to restore balance through active upward and downward motions. The analytical results demonstrate that the robot is able to recover from much larger disturbances using our proposed methods. Simulations of the simple point mass model validate our analysis. Besides, prototype controllers that incorporate our proposed strategies have also been implemented on a simulated humanoid robot. Numerical simulations on both the simple point mass model and the realistic humanoid model prove the effectiveness of proposed strategies.

KEYWORDS: Biped robot; Stability; Push recovery; Flexion; Vertical motion.

## 1. Introduction

Humanoid robots have been studied extensively in order to replace or assist humans in difficult tasks. They are expected to be robustly suitable for complex situations. Human legs can easily deal with some external disturbance in both walking and standing states; in contrast, artificial legged systems tend to be unreliable. Thus, more stable biped systems and control strategies are required for the further application of humanoid robots.[1] Similar to the human case, perturbation, as a common physical interaction between the robots and other factors such as the environment, is one of the most important perspectives for studying the balance ability of biped systems.

Consequently, balance control of biped systems has been studied for many years. Kajita *et al*.[2] presented a famous model called the Linear Inverted Pendulum Model (LIPM). This model treated the body of biped robots as a point mass moving at a constant height (see Fig. 2). Then, the humanoid motion was represented by a one-dimensional linear system that could be analytically solved.

Pratt *et al*.[3] introduced the concept of Capture Point and Capture Region. The capture point is the point on the ground where the robot can step towards in order to stop and restore balance. All possible capture points at a certain time form the capture region. Pratt also extended the LIPM by adding a flywheel on the robot body, and investigated the influence of the centroidal angular momentum in walking and standing states.

* Corresponding author. E-mail: fcl@tsinghua.edu.cn

Downloaded from https://www.cambridge.org/core. Shaanxi Normal University, on 01 Jul 2020 at 19:14:54, subject to the Cambridge Core terms of use, available at https://www.cambridge.org/core/terms. https://doi.org/10.1017/S0263574716000308

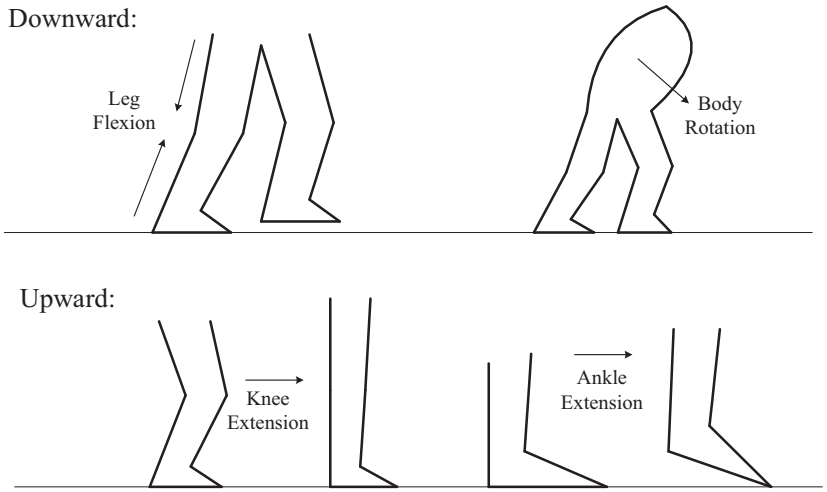


Fig. 1. Postures involving vertical motion when humans are disturbed.

Koolen *et al.*[4] further defined and obtained N-step capture points and capture regions based on the LIPM and its extension model. They also developed a control strategy based on the capturability theory[5] that enabled a M2V2 humanoid robot to walk and recover from omnidirectional push.

Hofmann[6] argued that maintaining the balance of a humanoid robot is to control the horizontal motion of the Center of Mass (CoM) of the robot. He summarized that human postures for maintaining balance can be classified into three different strategies involving ankle, torso and step. All of them are related to the shift of the Center of Pressure (CoP).

Some of those strategies were implemented on real and simulated humanoid robots. Boston Dynamics demonstrated that their biped robot Atlas can recover from a lateral disturbance by rotating its arms, trunk and leg.[7] Chen *et al.*[8] proposed an external acceleration detection and quadratic programming based controller for a force controllable humanoid robot. Fu[9] utilized an adaptive footstep updating strategy on a simulated humanoid robot in order to recover balance from perturbation during walking. In refs. [16], [17] and [19], disturbance rejection problems have been considered in the framework of sensory feedback control and passive walking theory.

Machine learning methods have also been applied to humanoid push recovery problems. Yi *et al.*[10] proposed a reinforcement learning method that integrates disturbance recovery strategies with a zero moment point based walking controller. Li *et al.*[11] used an artificial bee colony-learning algorithm as a center pattern generator to produce best gait patterns for humanoid robots.

Some researchers focused on human behaviors under external disturbances. Semwal *et al.*[12] proposed a bio-inspired eight-phase gait model based on the observation of humans. This eight-phase hybrid automata has been applied on a humanoid robot. Maus *et al.*[13] introduced the concept of the Virtual Pivot Point (VPP), and the stability of human beings results from the active manipulation of ground reaction forces in order to create a stable pendulum-like swinging motion.

Although many investigations on the stability of biped robots have been conducted, little attention has been paid on the vertical movement of the humanoid. In particular, a basic assumption of LIPM is that the CoM of the robot is kept at a constant height. However, human beings can move upward and downward actively in order to recover balance from external disturbances. As shown in Fig. 1, for the human case, leg flexion and body rotation motions would cause downward movement while knee extension and ankle extension would result in upward movement. When facing unexpected external disturbances, humans execute these postures accordingly in order to maintain balance.

In this paper, we show that the active vertical movement of the CoM could significantly increase the capture region and assist a biped robot to recover from external disturbances. Two strategies, namely, the flexion strategy and the extension strategy respectively corresponding to the downward and the upward motions, are proposed. The effectiveness of these strategies is demonstrated theoretically by the expansion of the capture region. The estimation results indicate that a biped robot is able to recover from 30%-50% larger external disturbances (represented by the CoM speed) when the

Downloaded from https://www.cambridge.org/core. Shaanxi Normal University, on 01 Jul 2020 at 19:14:54, subject to the Cambridge Core terms of use, available at https://www.cambridge.org/core/terms. https://doi.org/10.1017/S0263574716000308

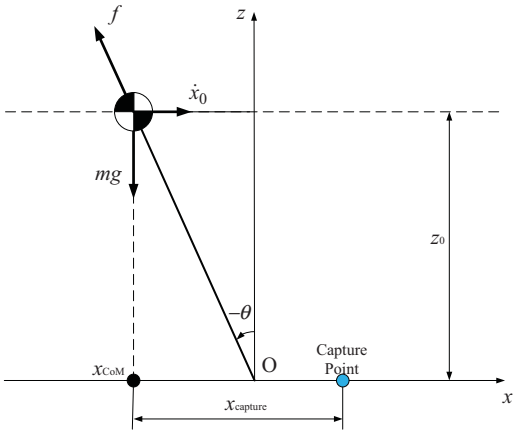


Fig. 2. Linear inverted pendulum model (LIPM) and capture point.[2]

proposed strategies are applied. Simulations on a simple point mass model and the comparison results of the capture point prove our analysis. A simple controller that incorporates our proposed strategies has also been designed for a small humanoid robot. The controller enables the robot to handle external disturbances, which would otherwise push the robot down to the ground when the proposed controller is not engaged.

The rest of this paper is organized as follows. In Section 2, a brief review on LIPM and the capture point is introduced. The flexion model, strategy and corresponding computations are presented in Section 3. The extension model, strategy and related computations are proposed in Section 4. In Section 5, we present how the capture point varies when changing parameters such as time, flexion acceleration and height of the robot. The numerical simulations are presented in Section 6, on both a simple point mass model and a realistic humanoid robot. The conclusions and future work are given in the last section.

## 2. Linear Inverted Pendulum Model (LIPM) and Capture Point

The balance recovery strategy presented in this paper is based on the concept of capture point and LIPM. In order to get a thorough understanding, we review some properties and principles of LIPM[2] and the concept of capture point[3] in this section.

Figure 2 shows the commonly used 2D (two-dimensional) LIPM model. It consists of a point mass and a massless, variable length leg that is in contact with the flat ground. The point mass is assumed to be at a constant height $z_0$. This indicates that the body has no vertical movement during locomotion.

The equations of motion for the body mass can be written as

$$\begin{aligned} f\sin(\theta) &= m\ddot{x}, \\ f\cos(\theta) &= mg, \end{aligned} \tag{1}$$

where $f$ is the supporting force of the leg, $x$ is the position of CoM, and $m$ is the mass of the point. Based on the geometric relation shown in Fig. 2, we can plug in $\theta = \tan^{-1}(x/z_0)$ and derive

$$\ddot{x} = \frac{g}{z_0}x. \tag{2}$$

Solving this equation with initial conditions, we get

$$x(t) = x_0\cosh(\omega t) + \frac{\dot{x}_0\sinh(\omega t)}{\omega}, \tag{3}$$

where $x_0$ is the initial position, $\dot{x}_0$ is the initial speed, and $\omega = \sqrt{g/z_0}$.

Downloaded from https://www.cambridge.org/core. Shaanxi Normal University, on 01 Jul 2020 at 19:14:54, subject to the Cambridge Core terms of use, available at https://www.cambridge.org/core/terms. https://doi.org/10.1017/S0263574716000308

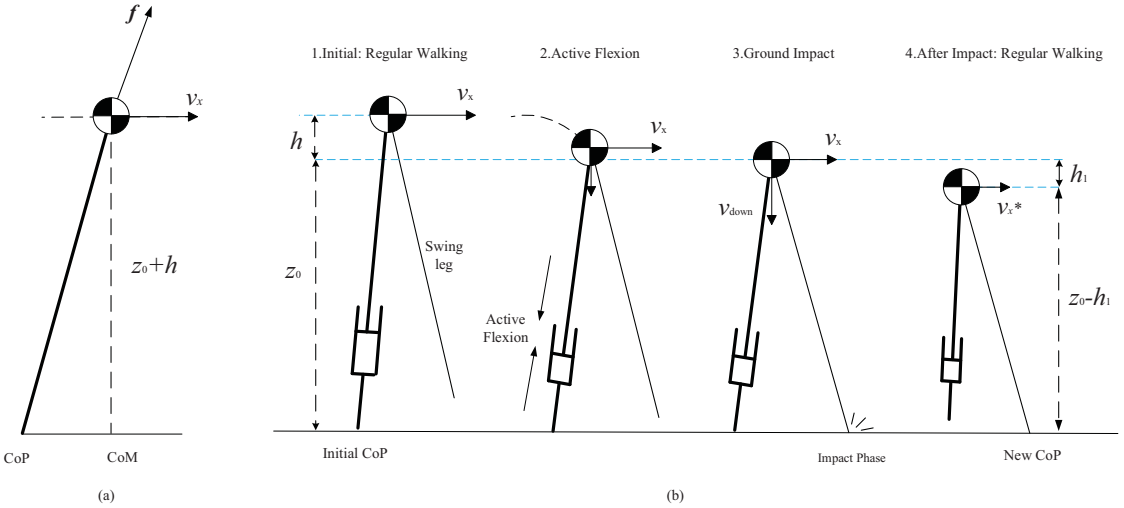


Fig. 3. Description of the proposed flexion strategy. (a) The flexion strategy can be applied to situations when the CoM is in front of the CoP. (b) Models and the general process of flexion strategy: In (b).2 and (b).3, the robot uses the active flexion motion to reduce the supporting force $f$, gain vertical velocity and utilize impact to dissipate excessive energy. In the figure, $h$ is the downward displacement caused by the flexion strategy, and $h_1$ is the downward displacement during the impact process.

The capture point, introduced in ref. [3], is the point on the ground that enables the robot to come to a stop if it were to place its step location there. Generally, it is difficult to solve the capture point for a complex biped robot. Hence, capture points of simplified models are preferred in robot dynamic control. The capture point of LIPM could be derived as follows.

In LIPM, there is a conserved quantity called the orbital energy:[3]

$$E_{\text{orb}} = \frac{1}{2}\dot{x}^2 - \frac{1}{2}\frac{g}{z_0}x^2. \tag{4}$$

If $E_{\text{orb}} = 0$, the point mass will stop on the support point, the state of robot is captured. By setting $E_{\text{orb}} = 0$, we have

$$x = \frac{\dot{x}}{\omega} \text{ or } x = -\frac{\dot{x}}{\omega}. \tag{5}$$

The above equation can represent a stable or an unstable state. If $x$ and $\dot{x}$ have opposite signs, the point mass is moving towards the supporting point and the state is stable. The foot placement can be placed at any point instantaneously since the legs are assumed to be massless. Therefore, the capture point of LIPM is

$$x_{\text{capture}} = \frac{\dot{x}}{\omega}.$$

## 3. Flexion Strategy and Capturability-Based Analysis

In this section, we focus on the flexion motion and its contribution to balance recovery from an external disturbance. Section 3.1 introduces the overall process and general idea. Sections 3.2 and 3.3 provide an integral estimation of the capture point with the flexion motion.

### *3.1. General idea and model description*

As shown in Fig. 3(a), suppose that the CoM of a biped system is in front of the CoP with a horizontal speed $v_x$. An external disturbance in the forward motion direction may exceed the capability of regular stepping method and thus push the robot falling to the forward direction. In order to avoid fall, additional strategy other than the normal stepping method should be considered. From the CoM point of view, the horizontal speed $v_x$ should be reduced or eliminated in the subsequent few steps. In

Downloaded from https://www.cambridge.org/core. Shaanxi Normal University, on 01 Jul 2020 at 19:14:54, subject to the Cambridge Core terms of use, available at https://www.cambridge.org/core/terms. https://doi.org/10.1017/S0263574716000308

this situation, the force $f$ provided by the supporting leg will further increase the horizontal speed, and make the balance restoring more difficult.

Hence, postures that minimize the supporting force $f$ should be adopted when the CoM is in front of the CoP. To this end, we propose a strategy that is referred to as the "flexion strategy" in the sequel. The overall process is illustrated in Fig. 3(b). Initially, the biped system has an increased speed $v_x$ resulting from a forward push. In (b).2 and (b).3, the biped system uses active flexion motion to reduce the supporting force $f$, gain vertical velocity $v_{\text{down}}$ and utilize impact to dissipate excessive energy. After the impact, the biped system will restore to the regular walking speed $v_x^*$, as shown in the Fig. 3(b).4.

The effectiveness of flexion strategy comes from the active utilization of the CoM downward motion and the ground impact to dissipate excessive kinetic energy. The proposed flexion strategy could be considered as a counterpart of the "push off" operation, whose purpose is to reduce the impact energy cost through active extension of the supporting leg.[18]

In ideal situation, the supporting leg is massless so that the supporting force can be eliminated by the flexion motion instantaneously. In practical situation that the leg of the biped system is not massless, the supporting force could also be eliminated if the flexion motion of the supporting leg is faster than free-fall. For the both situations, the CoM will perform free-fall motions with downward acceleration $g$. For most humanoid robots, the actuators might not be powerful enough to fully eliminate the supporting forces. This situation will be covered in our model hypothesis later.

Note that the supporting force is eliminated not only by the flexion of supporting legs, but also by the rotation of the body for the human beings (see Fig. 1). In this paper, we attribute all these postures into the vertical velocity term $v_{\text{down}}$.

In Sections 2.2 and 2.3, a simple point mass model is used to estimate the capture point of biped robots when the flexion strategy is incorporated. In particular, Section 2.2 focuses on the impact phase when the robot reduces its downward velocity caused by the flexion falling process. Section 2.3 will estimate the capture point as a function of time. Generally, the following model hypothesis will be used:

(1) The robot consists of a point mass and two massless legs.
(2) The gait of the walking can be divided into two phases: regular walking phase and height changing phase. In the regular walking phase, the robot follows the principles of LIPM.[2]
(3) During height changing phase, including the flexion process and the impact process, the magnitude of the vertical acceleration of the biped robot remains constant.

The third assumption above is an extension of LIPM, which holds zero vertical acceleration hypothesis. This constant vertical acceleration could be replaced by an average value in practice.

### *3.2. Instantaneous capture point estimation with downward velocity*

In this section, we will estimate the capture point of a simple point mass model with a horizontal velocity $v_x$ and a considerable downward velocity $v_{\text{down}}$, where $v_{\text{down}}$ results from the active downward motion process. In other words, we would analyze the process in which the robot reduces its downward velocity to zero, and we assume that the robot follows the principles of LIPM after this process, as shown in Fig. 4.

The common way to deal with ground impact is assuming the legs are quite powerful to stop the downward movement in an infinitesimal time period. In our approach, because of the active flexion motion, the downward speed considered here is much larger than the value during normal walking, and may lead to a longer impact period. Hence, in this paper, the impact is considered as a finite-time process.

In order to consider both the strength of the leg and the feasibility of analysis, we assume that the magnitude of the upward acceleration provided by the supporting leg is constant. Note that this magnitude describes the strength of the legs. Powerful legs are able to produce larger accelerations. This constant magnitude could be replaced by an average value in practice.

For convenience, as shown in Fig. 4, we use $z_0$ to denote the initial height when the swing leg touches the ground, $h_1$ is downward displacement during this process, $v_x$ and $v_{\text{down}}$ are the initial horizontal and vertical velocities, respectively, $v_x^*$ is the horizontal velocity after the impact.

Downloaded from https://www.cambridge.org/core. Shaanxi Normal University, on 01 Jul 2020 at 19:14:54, subject to the Cambridge Core terms of use, available at https://www.cambridge.org/core/terms. https://doi.org/10.1017/S0263574716000308

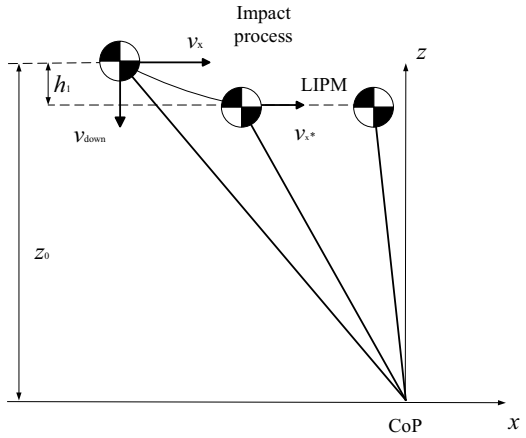


Fig. 4. The impact process of the biped robot.

Let $a$ denote the constant magnitude of the vertical acceleration during the impact process. Then, the equations of motion can be written as

$$\begin{aligned} \ddot{x} &= \tfrac{g+a}{z} x, \\ \ddot{z} &= a. \end{aligned} \tag{7}$$

Moreover, the initial conditions are

$$\begin{aligned} x_{t=0} &= x_0 \\ \dot{x}_{t=0} &= \dot{x}_0 \\ z_{t=0} &= z_0 \\ \dot{z}_{t=0} &= -v_{\text{down}} \end{aligned} . \tag{8}$$

First, we deal with the vertical motion. Since the vertical acceleration is constant $a$, we have

$$z(t) = z_0 - v_{\text{down}}\, t + \frac{1}{2} a\, t^2 . \tag{9}$$

When $t_1 = \frac{v_{\text{down}}}{a}$, $\dot{z}(t_1) = 0$. At the time $t_1$, the vertical displacement is

$$h_1 = -\frac{v_{\text{down}}\, t_1}{2}. \tag{10}$$

Next, we turn to the horizontal motion. Notice that in this process

$$\begin{aligned} z &\le z_0 \\ |\tfrac{g+a}{z}| &\ge |\tfrac{g+a}{z_0}|. \end{aligned} \tag{11}$$

Thus, we conservatively use the following equation

$$\ddot{x} = \omega_1^2 x, \tag{12}$$

where $\omega_1 = \sqrt{\frac{g+a}{z_0}}$, to estimate the speed and the position of the robot. By using the approximation (12), the capture point we estimate will be a little bit larger. Please refer to Appendix A for detailed analysis. From Eq. (12), we can derive

$$\begin{aligned} x(t) &= x_0 \cosh(\omega_1 t) + \tfrac{\dot{x}_0}{\omega_1} \sinh(\omega_1 t), \\ \dot{x}(t) &= \omega_1 x_0 \sinh(\omega_1 t) + \dot{x}_0 \cosh(\omega_1 t). \end{aligned} \tag{13}$$

Downloaded from https://www.cambridge.org/core. Shaanxi Normal University, on 01 Jul 2020 at 19:14:54, subject to the Cambridge Core terms of use, available at https://www.cambridge.org/core/terms. https://doi.org/10.1017/S0263574716000308

To derive the capture point, we need $x(t_1)$ to be the capture point of $\dot{x}(t_1)$. By using the following relationship, which was presented in ref. [2],

$$x\left(t_1\right) = \omega_0' \dot{x}\left(t_1\right), \tag{14}$$

where $\omega_0' = \sqrt{\frac{g}{z_0 - h_1}}$, we can derive

$$\begin{array}{l} x_0 = \lambda_1 \frac{\dot{x}_0}{\omega'_0}, \\ \lambda_1 = \frac{1+\frac{\omega_0}{\omega_1}\tanh(\omega_1 t_1)}{1+\frac{\omega_1}{\omega_0}\tanh(\omega_1 t_1)}, \text{ and } \omega'_0 = \sqrt{\frac{g}{z_0 - h_1}} = \omega_0 \sqrt{\frac{z_0}{z_0 - h_1}}, \end{array} \tag{15}$$

where $\omega_0 = \sqrt{\frac{g}{z_0}}$, $\omega_1 = \sqrt{\frac{g+a}{z_0}}$. Then, the capture point is

$$x_{\text{capture}} = \lambda\, x_{\text{capture0}}, \tag{16}$$

where $\lambda = \lambda_1 \sqrt{\frac{z_0 - h_1}{z_0}}$, and $x_{\text{capture0}} = \frac{\dot{x}}{\omega_0}$ is the initial capture point without the vertical velocity. Hence, we provide an expression for the capture point of the simple point mass model with considerable vertical movement. This lays foundation for our further analysis.

### *3.3. Time-dependent estimation of the capture point*

In this section, we analyze the flexion process, in which the active flexion motion is executed before the swing leg touches the ground. Time-dependent computation of the capture point will be provided.

In the flexion strategy, although the supporting force provided by the supporting leg could be very complicated before the swing leg touches the ground, we only concern about the final conditions: final horizontal position, final horizontal velocity, final height and final vertical velocity. Consequently, we will only analyze a simple but representative situation, in which the downward acceleration's magnitude is kept as a constant. Note that this magnitude describes the strength of the legs. Powerful legs are able to produce a faster flexion motion, which corresponds to a larger vertical acceleration and a faster final vertical speed. For complex situations where the vertical force given by the supporting leg is not constant, the analysis is almost the same provided that the final velocity and position are predictable.

By using $a_h$ to denote the constant magnitude of downward acceleration, and $h$ to denote the vertical displacement in flexion process shown in Fig. 3, equations of the vertical motion can be expressed as

$$v_{\text{down}} = -\sqrt{2a_h h} = -a_h t, \; h = -\frac{1}{2} a_h t^2. \tag{17}$$

As shown in Fig. 3(b), before the swing leg touches the ground, it is clear that

$$z_0 \geq z \geq z_0 - h. \tag{18}$$

By using an approximation method similar to that expressed in Eq. (12) and plugging Eq. (18), we can show that the horizontal acceleration satisfies the following relationship

$$\ddot{x} = \frac{a_h}{z} x \leq \frac{a_h}{z_0 - h} x. \tag{19}$$

By considering, the initial conditions and using the theorem presented in Appendix A, we can get an upper bound for the horizontal velocity as follows

$$\dot{x}\left(t\right) \leq \omega_2 x_0 \sinh\left(\omega_2 t\right) + \dot{x}_0 \cosh\left(\omega_2 t\right), \tag{20}$$

where $\omega_2 = \sqrt{\frac{a_h}{z_0 - h}}$.

Downloaded from https://www.cambridge.org/core. Shaanxi Normal University, on 01 Jul 2020 at 19:14:54, subject to the Cambridge Core terms of use, available at https://www.cambridge.org/core/terms. https://doi.org/10.1017/S0263574716000308

Analogous to the instantaneous case in Section 3.2, by extending Eq. (16), we can get the time-dependent estimation of the capture point as follows

$$x_{\text{capture}}(t) = x_{\text{capture0}}(t)\,\lambda\left(v_{\text{down}}(t), z(t)\right), \tag{21}$$

where $x_{\text{capture0}}(t) = \dot{x}(t)\sqrt{z(t)/g}$ is the instantaneous capture point without considering the vertical velocity, the upper bound of $\dot{x}(t)$ is given in Eq. (20); $v_{\text{down}}(t)$ and $z(t)$ are the vertical velocity and the vertical height given in Eq. (17), respectively; the term $\lambda(v_{\text{down}}(t), z(t))$ in Eq. (21) can be calculated in a way similar to the case shown in Eq. (16).

Specially, if $a_h = g$, i.e., the CoM is experiencing a free-fall motion, then, the accelerations are

$$\begin{aligned} \ddot{x}_{\text{freefall}} &= 0, \\ \ddot{z}_{\text{freefall}} &= -g. \end{aligned} \tag{22}$$

Plugging the initial conditions, the velocity can be computed as follows:

$$\begin{aligned} v_{\text{x-freefall}}(t) &= \dot{x}_0, \\ v_{\text{down-freefall}}(t) &= -gt. \end{aligned} \tag{23}$$

For any other possible $x(t)$ and $z(t)$ with non-zero supporting force, the equations of motion are

$$\begin{aligned} \ddot{x} &= \tfrac{f}{m}\sin(\theta), \\ \ddot{z} &= -g + \tfrac{f}{m}\cos(\theta), \end{aligned} \tag{24}$$

where $\theta = \tan^{-1}(\frac{x}{z})$, $x > 0$, $z > 0$, and $f \geq 0$. We can conclude that

$$\begin{aligned} \ddot{x} &\geq 0 = \ddot{x}_{\text{freefall}}, \\ \ddot{z} &\geq -g = \ddot{z}_{\text{freefall}}. \end{aligned} \tag{25}$$

Using the theorem shown in the Appendix A, we can get a lower bound for the horizontal velocity

$$\dot{x}(t) \geq \dot{x}_0, \tag{26}$$

and lower bounds for the vertical displacement and the vertical velocity

$$\begin{aligned} z(t) &\geq z_0 - \tfrac{1}{2}gt^2, \\ \dot{z}(t) &\geq -gt. \end{aligned} \tag{27}$$

All the inequalities in Eq. (27) become equalities if and only if $f = 0$. Hence, we can conclude that the free-fall flexion strategy can achieve minimum horizontal velocity, maximum downward velocity and downward displacement (notice that the vertical displacement and the vertical velocity are negative algebraically) before the swing leg touches the ground.

## 4. Extension Strategy and Capturability-Based Analysis

### *4.1. General idea and model description*

As shown in Fig. 5(a), the biped system has an increased velocity $v_x$ caused by an external push in the forward direction when the CoP is in front of the CoM. This increased velocity might lead to the dangerous falling down with normal walking strategy. In order to ensure locomotion safety, the extension strategy other than normal stepping should be considered.

The supporting force $f$ that is provided by the supporting leg can reduce the horizontal velocity and mitigate the dangerous falling towards the forward direction. Our proposed extension strategy takes advantage of this fact and uses postures that maximize the effectiveness caused by the supporting

Downloaded from https://www.cambridge.org/core. Shaanxi Normal University, on 01 Jul 2020 at 19:14:54, subject to the Cambridge Core terms of use, available at https://www.cambridge.org/core/terms. https://doi.org/10.1017/S0263574716000308

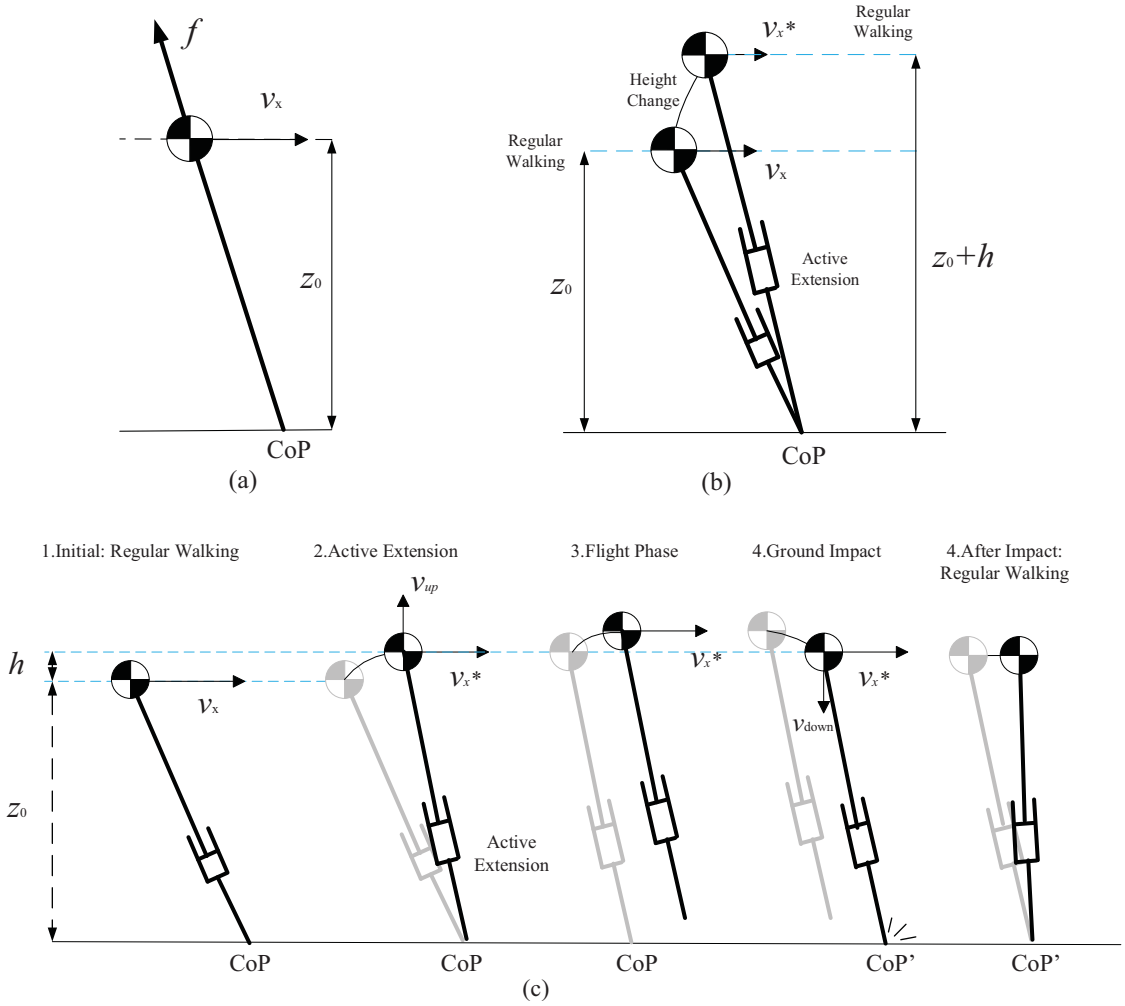


Fig. 5. Descriptions of the proposed extension strategy. (a) The extension strategy can be applied to situations that the CoP is in front of the CoM. (b) Extension strategy for the case of fixed CoP. (c) Process of extension strategy with flight phase: with the help of the flight phase and the ground impact, the excessive kinetic energy could be further dissipated. In the figure, $h$ is the upward displacement caused by the extension motion.

force $f$, as shown in Figs. 5(b) and (c). From the perspective of vertical motion, increasing the ground reaction force $f$ will make the robot "kick" the ground and lift its CoM upward actively. In fact, this strategy can be considered as the counterpart of the flexion strategy proposed in Section 3.

Figure 5(b) depicts the extension strategy for the case when the supporting foot is fixed on the ground. If the upward velocity of the CoM is considerably large, the robot might leave the ground and move with like a projectile, as shown in Fig. 5(c). In this case, with the help of the flight phase and ground impact, excessive kinetic energy can be further dissipated. In the following subsections, we will show two upward extension strategies that will increase the capture region and assist the biped robot to recover from external disturbances.

In Section 4.2, the capture point of the extension strategy with fixed supporting point is estimated. Section 4.3 will deal with the capture point of extension strategy with flight phase. In the subsequent sections, the following model hypothesis will be used:

(1) The robot consists of a point mass and two massless legs.
(2) The gait of the robot can be divided into two phases: the regular walking phase and height-changing phase. In the regular walking phase, the robot follows the principles of LIPM.[2]
(3) During the height changing phase of the proposed extension strategy, the vertical acceleration is a piecewise constant function.

Downloaded from https://www.cambridge.org/core. Shaanxi Normal University, on 01 Jul 2020 at 19:14:54, subject to the Cambridge Core terms of use, available at https://www.cambridge.org/core/terms. https://doi.org/10.1017/S0263574716000308

It should be noticed that the direction of vertical acceleration will change in the process because the initial vertical velocity and final vertical velocity are both zero.

*4.2. Capturability-based analysis of the extension strategy with fixed CoP*

In this section, we estimate the capture point of biped systems with extension strategy and fixed CoP (Fig. 5(b)). If the upward motion process is completed before the CoM passes the CoP, which will be true if the robot recovers from the initial speed, the capture point is just the instantaneous capture point.

The equations of motion are

$$\begin{aligned} \ddot{x} &= \frac{g+a}{z}x, \\ \ddot{z} &= a \end{aligned} \tag{28}$$

Analogous to the flexion case shown in Section 3, we first focus on the vertical motion. As explained in Section 4.1, the magnitude of the vertical acceleration is assumed to be constant. Because the initial vertical velocity and the final vertical velocity are both zero, we have

$$a = \begin{cases} a_0 & 0 < t < t_1 \\ -a_0 & t_1 < t < 2t_1 \end{cases} \quad t_1 = \sqrt{\frac{h}{g}}, \tag{29}$$

where $h$ is the possible rising height. Obviously, $a_0 < g$ when $t_1 < t < 2t_1$. At time $t = t_1$, the vertical displacement is $h/2$. Now, we turn to the horizontal motion, the equations of motion are

$$\begin{aligned} \ddot{x} &= \frac{g+a_0}{z}x \quad 0 < t < t_1 \\ \ddot{x} &= \frac{g-a_0}{z}x \; t_1 < t < 2t_1 \end{aligned} \quad . \tag{30}$$

Note that when $0 < t < t_1$, the horizontal acceleration is larger than the value of LIPM, which means that the extension strategy can help to recover balance from disturbance in this period. While for $t_1 < t < 2t_1$, the acceleration is smaller than that of LIPM, i.e., it is negative. Moreover, we have

$$\begin{aligned} z \le z_0 + \frac{h}{2}\left|\frac{g+a_0}{z}\right| &\ge \left|\frac{g+a_0}{z_0 + h/2}\right| \; 0 < t < t_1 \\ z \ge z_0 + \frac{h}{2}\left|\frac{g+a_0}{z}\right| &\le \left|\frac{g+a_0}{z_0 + h/2}\right| \; t_1 < t < 2t_1 \end{aligned} \quad . \tag{31}$$

Thus, we conservatively replace $z$ by $z_1 = z_0 + h$ to estimate the horizontal velocity. By using this approximation, the calculated horizontal speed is a little bit larger. Therefore, the capture point we get is still a little bit longer. The analysis of this statement is shown in Appendix A. After the substitution, we can solve the equations and derive the following

$$\begin{aligned} x(t) &= x_0 \cosh(\omega_1 t) + \frac{\dot{x}_0}{\omega_1}\sinh(\omega_1 t) \\ \dot{x}(t) &= \omega_1 x_0 \sinh(\omega_1 t) + \dot{x}_0 \cosh(\omega_1 t) \end{aligned} \quad 0 < t < t_1, \tag{32}$$

where $\omega_1 = \sqrt{\frac{g+a_0}{z_1}}$. Let $x_1$ and $\dot{x}_1$ denote the respective position and velocity at time $t_1$, the equations of motion for the time period $t_1 < t < 2t_1$ are

$$\begin{aligned} x(t) &= x_1 \cosh[\omega_2(t-t_1)] + \frac{\dot{x}_1}{\omega_2}\sinh[\omega_2(t-t_1)] \\ \dot{x}(t) &= \omega_2 x_1 \sinh[\omega_2(t-t_1)] + \dot{x}_1 \cosh[\omega_2(t-t_1)] \end{aligned} \quad t_1 < t < 2t_1, \tag{33}$$

Downloaded from https://www.cambridge.org/core. Shaanxi Normal University, on 01 Jul 2020 at 19:14:54, subject to the Cambridge Core terms of use, available at https://www.cambridge.org/core/terms. https://doi.org/10.1017/S0263574716000308

where $\omega_2 = \sqrt{\frac{g-a_0}{z_1}}$. If the robot is stable, the position and velocity at time $t = 2t_1$ is the capture point of LIPM,

$$x(t_1) = \omega'_0\, \dot{x}(t_1), \tag{34}$$

where $\omega'_0 = \sqrt{\frac{g}{z_0+h}}$. Solving these equations, we can get the capture point as follows

$$\begin{aligned} x_{\text{capture}} &= \lambda_2\, x_{\text{capture0}}, \\ \lambda_2 &= \sqrt{\frac{z_0}{z_0+h}}\frac{1+\dfrac{\omega_0}{\omega_1}\tanh(\omega_1 t_1)+\dfrac{\omega_0}{\omega_2}\tanh(\omega_2 t_1)+\dfrac{\omega_2}{\omega_1}\tanh(\omega_1 t_1)\tanh(\omega_2 t_1)}{1+\dfrac{\omega_1}{\omega_0}\tanh(\omega_1 t_1)+\dfrac{\omega_2}{\omega_0}\tanh(\omega_2 t_1)+\dfrac{\omega_2}{\omega_1}\tanh(\omega_1 t_1)\tanh(\omega_2 t_1)}, \end{aligned} \tag{35}$$

where $\omega_0 = \sqrt{\frac{g}{z_0}}$, and $x_{\text{capture0}} = \frac{\dot{x}_0}{\omega_0}$ is the initial capture point before applying the extension strategy.

### *4.3. Capturability-based analysis of the extension strategy with flight phase*

As shown in Fig. 5(c), the CoP of a biped system might move to a new supporting point with the CoM moving in a projectile motion, especially with the help of a significant upward velocity introduced by the extension strategy. In this subsection, we analyze the capture point of this case and show the contribution of the extension strategy to the disturbance rejection of biped system.

In the flight phase, although the swing leg is possible to swing about the CoM, in this subsection, we only deal with the simplest situation for which the swing leg is static about the CoM. The analysis for other complex situations is almost the same provided that the swing motion of leg is predictable.

In the upward acceleration phase, the equations of motion are

$$\begin{aligned} \ddot{x} &= \tfrac{g+a}{z}x, \\ \ddot{z} &= a. \end{aligned} \tag{36}$$

Applying an approximation method similar to that in Eq. (23), and replacing $z$ with $z_1 = z_0 + h$, where $h$ is the change of height before the supporting point leaves the ground in Fig. 5(c), we have

$$\ddot{x} = {\omega_1}^2\, x, \tag{37}$$

where $\omega_1 = \sqrt{\frac{g+a_0}{z_1}}$. Note that the horizontal velocity and displacement computed by this approximation are overestimated by the theorem in Appendix A. Hence, the corresponding capture point will be a little bit larger. Solving these equations with initial conditions, we get

$$\begin{aligned} x(t) &= x_0\cosh(\omega_1 t) + \frac{\dot{x}_0}{\omega_1}\sinh(\omega_1 t) \\ \dot{x}(t) &= \omega_1 x_0 \sinh(\omega_1 t) + \dot{x}_0\cosh(\omega_1 t) \end{aligned} \qquad 0 < t < t_1\,. \tag{38}$$

During the flight phase, the horizontal speed is kept constant while the vertical velocity is reversed downward. The distance between the CoM and the CoP is just $x(t_1)$. Under the assumption that the swing leg is static about the CoM in the flight phase, $x(t_1)$ will always represent the distance between the CoM and the CoP. Thus, $x(t_1)$ ought to be the capture point of $\dot{x}(t_1)$ with downward velocity $\dot{z}$. Analogous to Eq. (21) shown in Section 3, we can get the estimated capture point as

$$x(t_1) = \lambda(\dot{z})\, x_{\text{capture0}} = \frac{\lambda(\dot{z})}{\omega'_0}\dot{x}(t_1), \tag{39}$$

where $\omega'_0 = \sqrt{\frac{g}{z_{\text{final}}}}$, $z_{\text{final}}$ denotes the height when the swing leg touches the ground, as shown in the fourth step of Fig. 5(c). According to the previous assumption that the swing leg is static about the

Downloaded from https://www.cambridge.org/core. Shaanxi Normal University, on 01 Jul 2020 at 19:14:54, subject to the Cambridge Core terms of use, available at https://www.cambridge.org/core/terms. https://doi.org/10.1017/S0263574716000308

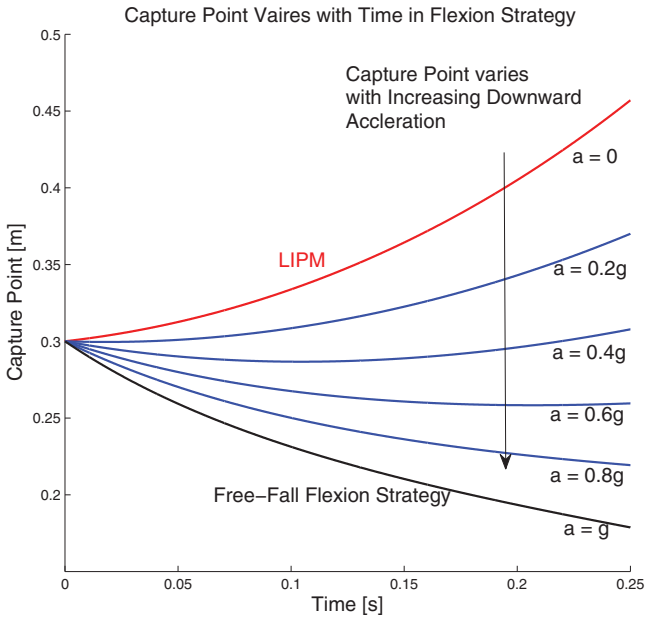


(a)

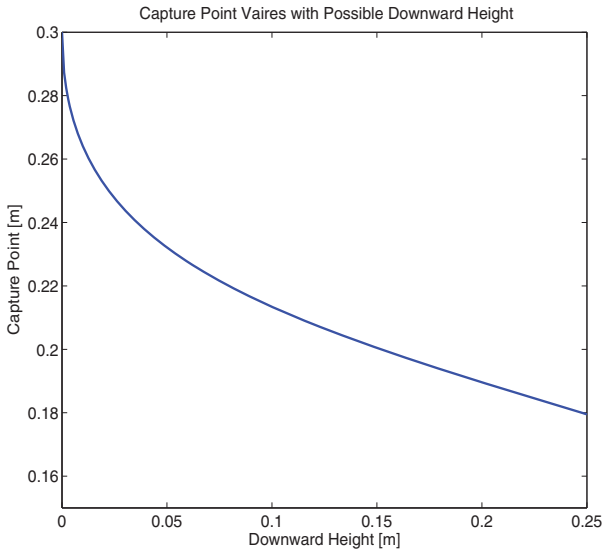


(b)

Fig. 6. (a) The capture point of the biped robot varies with time $t$ in the flexion leg strategy, where $a$ is the downward acceleration during the flexion process. Larger $a$ means stronger legs and faster flexion motions. (b) The capture point of biped robot varies with possible downward height in the flexion strategy.

CoM during the flight phase, we have $z_{\text{final}} = z_1$. Solving these equations, we can obtain the capture point of the extension strategy with flight phase as follows

$$x_{\text{capture}} = x_{\text{capture0}} \frac{\sinh(\omega_1 t_1)\,\omega'_0 / \omega_1 + \lambda \cosh(\omega_1 t_1)}{\cosh(\omega_1 t_1) + \lambda \sinh(\omega_1 t_1)\,\omega_1 / \omega'_0} \sqrt{\frac{z_0}{z_{\text{final}}}}, \tag{40}$$

where $x_{\text{capture0}} = \frac{\dot{x}(0)}{\omega_0}$ is the initial capture point before applying the extension strategy, $\omega_0 = \sqrt{\frac{g}{z_0}}$, and $\lambda$ is the term for which the expression is shown in Eq. (16).

Downloaded from https://www.cambridge.org/core. Shaanxi Normal University, on 01 Jul 2020 at 19:14:54, subject to the Cambridge Core terms of use, available at https://www.cambridge.org/core/terms. https://doi.org/10.1017/S0263574716000308

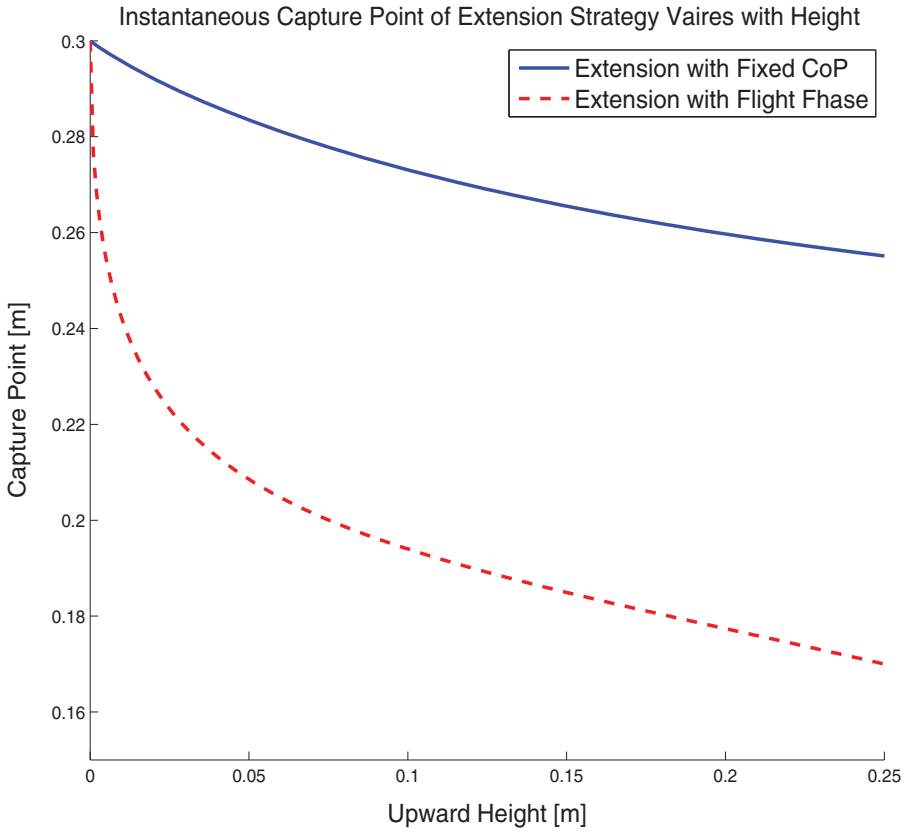


Fig. 7. The capture point of the biped robot varies with possible upward height when using the extension strategy.

### *4.4. Multi-step capturability and composite strategy*

In Sections 3 and 4, we describe two main types of strategies, which are named as the flexion strategy and the extension strategy, respectively. They are used in the situations when the CoM is placed behind/in front of the CoP, respectively. These two strategies can be combined into a composite strategy by considering the fact that the relative position of the CoP and the CoM changes periodically in a multi-step case. In addition, the vertical motions of the CoM introduced by these two strategies are opposite. Therefore, these two strategies can be applied alternately.

In our theoretical analysis, the robot is assumed to follow the LIPM except the height-changing period. Thus, the capture point for the composite strategy can be simply calculated by multiplying the coefficients for the extension strategy and flexion strategy, as follows

$$x_{\text{capture}} = (\lambda_{\text{flexion}}\, \lambda_{\text{extension}})\, x_{\text{capture0}}\,. \tag{41}$$

## 5. Parameter Variations of the Proposed Strategies and Models

Figure 6 shows the plots of the robot capture points as functions of time $t$ and possible downward height $h$, respectively, when the flexion strategy is applied. The initial speed is set to be 1 m/s, the initial height $z_0 = 1$ m, and the initial position $x_0 = 0.05$ m about the supporting point. In Fig. 6(a), the downward acceleration $a$ for the flexion process varies from 0 m/s$^2$ (LIPM) to $g$ (free-fall flexion strategy). Larger $a$ corresponds to stronger legs and faster flexion motions. From Fig. 6, we see that the capture point decreases significantly in comparison with the capture point of LIPM, which means a larger capture region is obtained and the robot is able to recover from larger initial speeds. Besides, one can see that the instantaneous capture point of LIPM is the upper bound of all possible capture points at any time, and the capture point for the free-fall flexion strategy is the lower bound.

Downloaded from https://www.cambridge.org/core. Shaanxi Normal University, on 01 Jul 2020 at 19:14:54, subject to the Cambridge Core terms of use, available at https://www.cambridge.org/core/terms. https://doi.org/10.1017/S0263574716000308

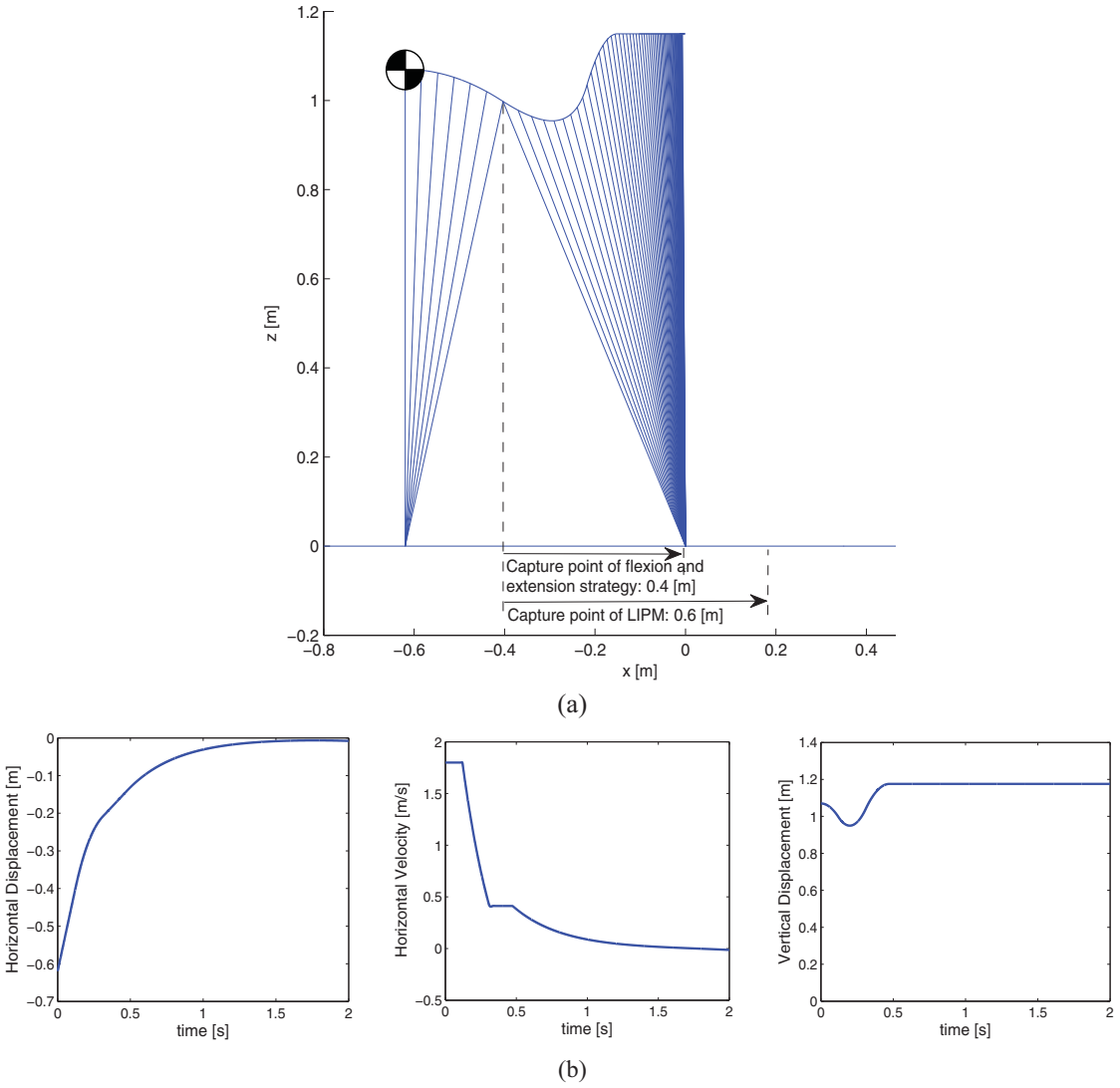


Fig. 8. (a) Spatial trajectories of the point mass model using the composite strategy consisting of the proposed flexion and extension strategies. (b) Simulation results. The robot has an initial horizontal velocity of 1.8 m/s.

Figure 7 shows that the robot's instantaneous capture point varies with possible upward height when the extension strategy is applied. The blue solid line is the case of fixed supporting point, and red dashed line is the case with flight phase. In the figure, the initial speed is 1 m/s, the initial height is 1 m, and the initial position $x_0 = -0.20$ m about the CoP. One can see that the capture point decreases (which indicates a larger capture region) significantly with respect to the upward height. The robot is able to recovery from larger initial speed when using large upward height.

## 6. Simulations and Results

### *6.1. Simulations of the simple point mass model*

The simple point mass model consists of a point mass and two massless legs. The length of legs is changeable. Similar to the analysis in Sections 2 and 3, the magnitude of the upward acceleration provided by the supporting legs is set to be a constant $a_0 = 15$ m/s$^2$. The downward acceleration of the CoM in falling stage is $g$. This means the flexion motion of the supporting leg is fast enough to fully cancel out the supporting force. The initial height of the CoM is 1.06 m. The simulations are performed on Matlab platform.

Downloaded from https://www.cambridge.org/core. Shaanxi Normal University, on 01 Jul 2020 at 19:14:54, subject to the Cambridge Core terms of use, available at https://www.cambridge.org/core/terms. https://doi.org/10.1017/S0263574716000308

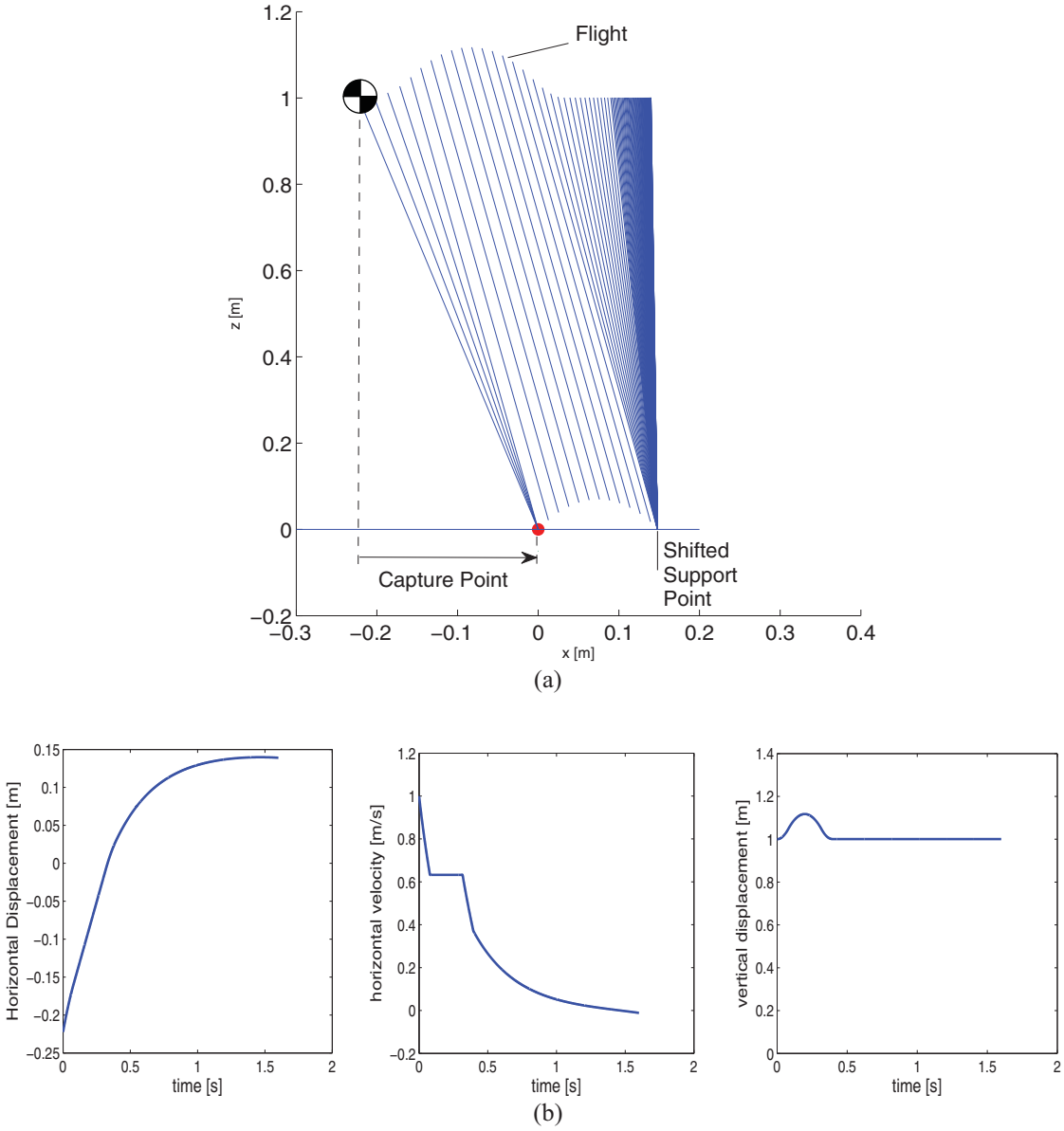


Fig. 9. (a) Spatial trajectories of the point mass model using the extension strategy with flight phase. (b) Simulation results. The robot has an initial horizontal velocity of 1 m/s.

Figure 8(a) presents the stick figure of the biped robot using the composite strategy consisting of our proposed flexion and extension strategies to recover from a large initial speed, which is set to be 1.8 m/s. The spatial trajectories of the supporting legs and the robot CoM are presented in Fig. 8(a). Figure 8(b) shows the time trajectories of the horizontal displacement, horizontal velocity and vertical displacement. As shown in Fig. 8(a), the capture point is reduced from 0.6 m to 0.4 m by combining the flexion and the extension strategy. This verifies the idea that flexing the rear leg and extending the leading leg can help to decelerate the robot and avoid falling down.

Figure 9(a) presents the stick figure of the biped robot using the proposed extension strategy with flight phase to recover from an initial speed. In this simulation, the robot CoM moves like a projectile when the upward velocity of the CoM is 1 m/s with the extension strategy. The initial position of the CoM is approximately $-0.22$ m relative to the supporting point. The initial horizontal velocity is 1 m/s. As shown in Fig. 9(b), the horizontal velocity of the robot is decreased by extending the supporting leg while the CoM is behind the CoP.

Downloaded from https://www.cambridge.org/core. Shaanxi Normal University, on 01 Jul 2020 at 19:14:54, subject to the Cambridge Core terms of use, available at https://www.cambridge.org/core/terms. https://doi.org/10.1017/S0263574716000308

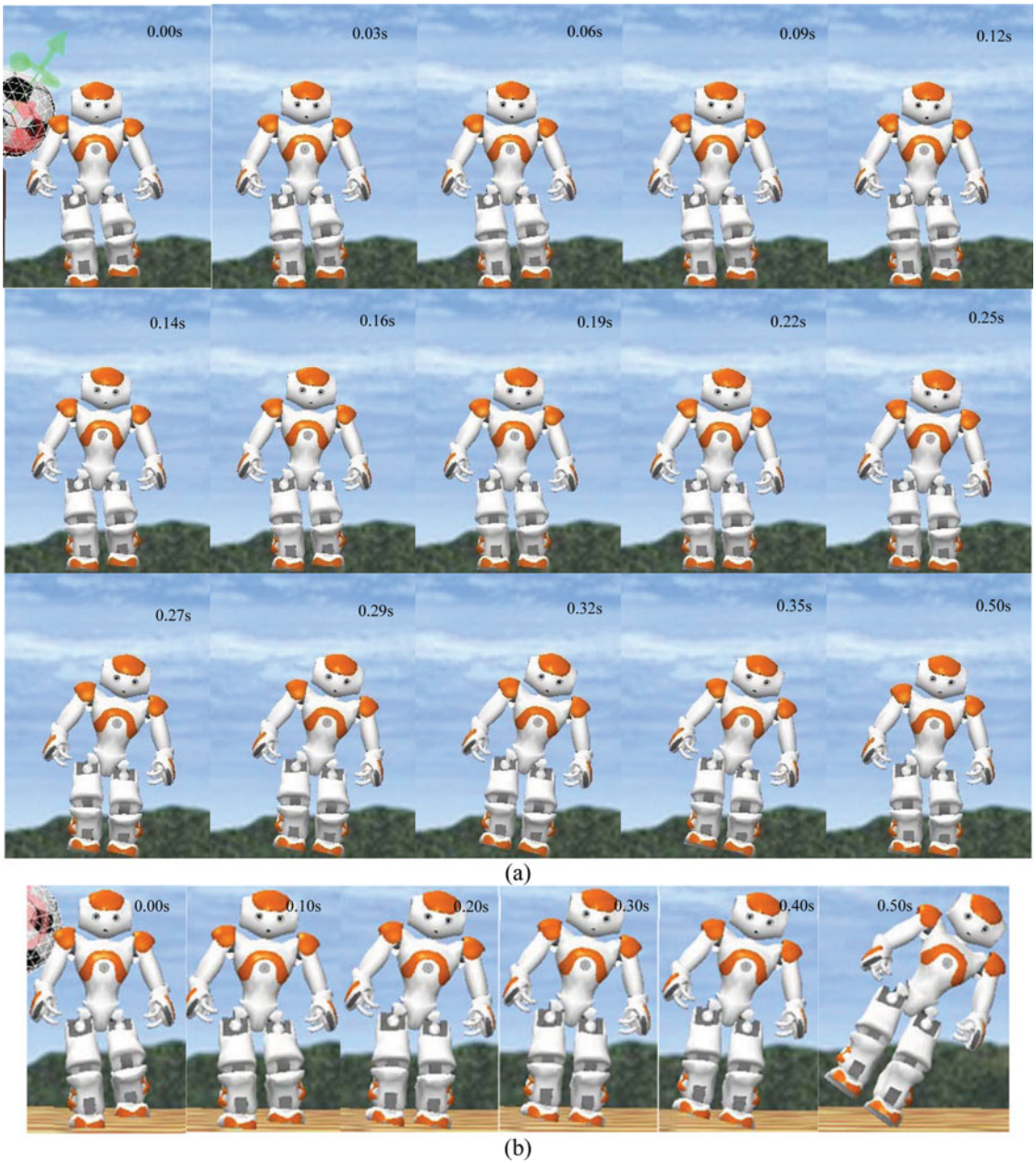


Fig. 10. (a) Image sequences showing that the robot recovers from a lateral push by using the proposed flexion strategy in single support state. (b) Image sequences showing that the robot falls down without flexion strategy under the same external disturbance.

### *6.2. Humanoid robot simulations*

To demonstrate the extendibility and effectiveness of our proposed strategies, simulation studies have also been performed on a small humanoid robot. The humanoid robot is implemented by Aldebaran[14] and the simulation software is developed by Cyberbotics.[15] In the simulations, a ball is used to hit the robot, providing the external disturbance. A simple controller incorporated with our strategies is applied to the simulated robot. Comparative experiments are conducted to prove the effectiveness of our proposed strategies.

Figure 10(a) shows the case that the robot recovers from a lateral push by using the proposed flexion strategy in a single support state. In this simulation, the robot is initially posed into a single support state, which is common and relatively unstable for humanoid robots. Then, a lateral push

Downloaded from https://www.cambridge.org/core. Shaanxi Normal University, on 01 Jul 2020 at 19:14:54, subject to the Cambridge Core terms of use, available at https://www.cambridge.org/core/terms. https://doi.org/10.1017/S0263574716000308

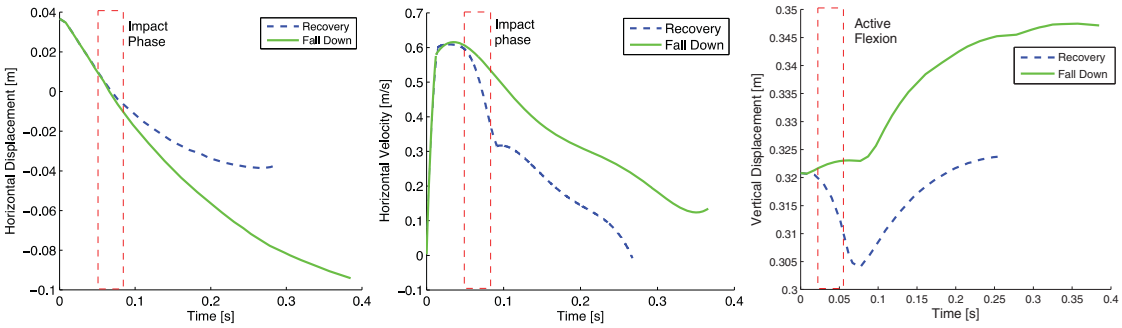


Fig. 11. The horizontal displacement, horizontal velocity and vertical displacement trajectories of the robot CoM with/without using the proposed flexion strategy.

(introduced by the impact of a ball from the lateral direction) is applied to the robot. The robot flexes its supporting leg while taking its swing leg a step in the lateral direction to regain balance. As a comparison, we apply the same external disturbance to the robot but deactivate the flexion movement of supporting leg (Fig. 10(b)). In this case, only a lateral step is taken by the robot in order to recover from the external disturbance. The robot eventually falls down. The comparison shows the effectiveness of the flexion strategy. Please refer to the Electronic Annex 2 in Appendix B for the video clip of this simulation.

Figure 11 shows the trajectories of the horizontal displacement, horizontal velocity and vertical displacement of the CoM with/without using the proposed flexion strategy. From the vertical displacement trajectory, the robot with the proposed flexion strategy uses active flexion of its supporting leg to gain downward velocity and displacement, which leads to impact phase shown in horizontal velocity trajectory and prevent its falling. On the contrary, the robot without using the proposed strategy will eventually falls down, as it does not have the flexion and impact process generated by active flexion strategy as shown in Fig. 11.

Figure 12(a) shows the case that the robot recovers from a push in the forward direction by using the proposed extension strategy with flight phase in its double support state. The robot is initially set at its "initial stand" state. Then, a forward push (hit by a ball from the back) is applied. The robot actively moves upward, uses flight phase and ground impact to restore balance. For comparison purposes, we apply the same external disturbance to the robot but deactivate the extension motion, as shown in Fig. 12(b). In this case, the robot falls down eventually.

Figure 12(c) shows the simulated results of the horizontal displacement, horizontal velocity and vertical displacement trajectories of the robot CoM. As shown in the figure, by using the proposed extension strategy, the robot actively extends its legs and moves upward, uses flight phase and the ground impact to regain balance. In contrast, the robot will eventually fall down without using our extension strategy. Both the horizontal and the vertical motions of the robot are significantly different when the proposed strategy is applied. These results prove the effectiveness of our proposed extension strategy for the case with flight phase. Please refer to the Electronic Annex 2 in Appendix B for the video clips of this simulation.

## 7. Conclusion and Future Work

In this paper, we investigate the active vertical motion of biped systems and its significance to the balance of biped robots. This vertical motion has been commonly neglected in the well-known model called the Linear Inverted Pendulum Model. Two strategies named the flexion strategy and the extension strategy are proposed. Theoretical estimation of the capture point corresponding to these two strategies is derived using a simple point mass model. Simulations on a simple model and the comparison results against the LIPM method prove our analysis. In addition, simple controllers incorporating our proposed strategies are implemented on a simulated humanoid robot to help the robot for better handling of external disturbances that would otherwise (i.e., proposed strategies deactivated) push down the robot.

Downloaded from https://www.cambridge.org/core. Shaanxi Normal University, on 01 Jul 2020 at 19:14:54, subject to the Cambridge Core terms of use, available at https://www.cambridge.org/core/terms. https://doi.org/10.1017/S0263574716000308

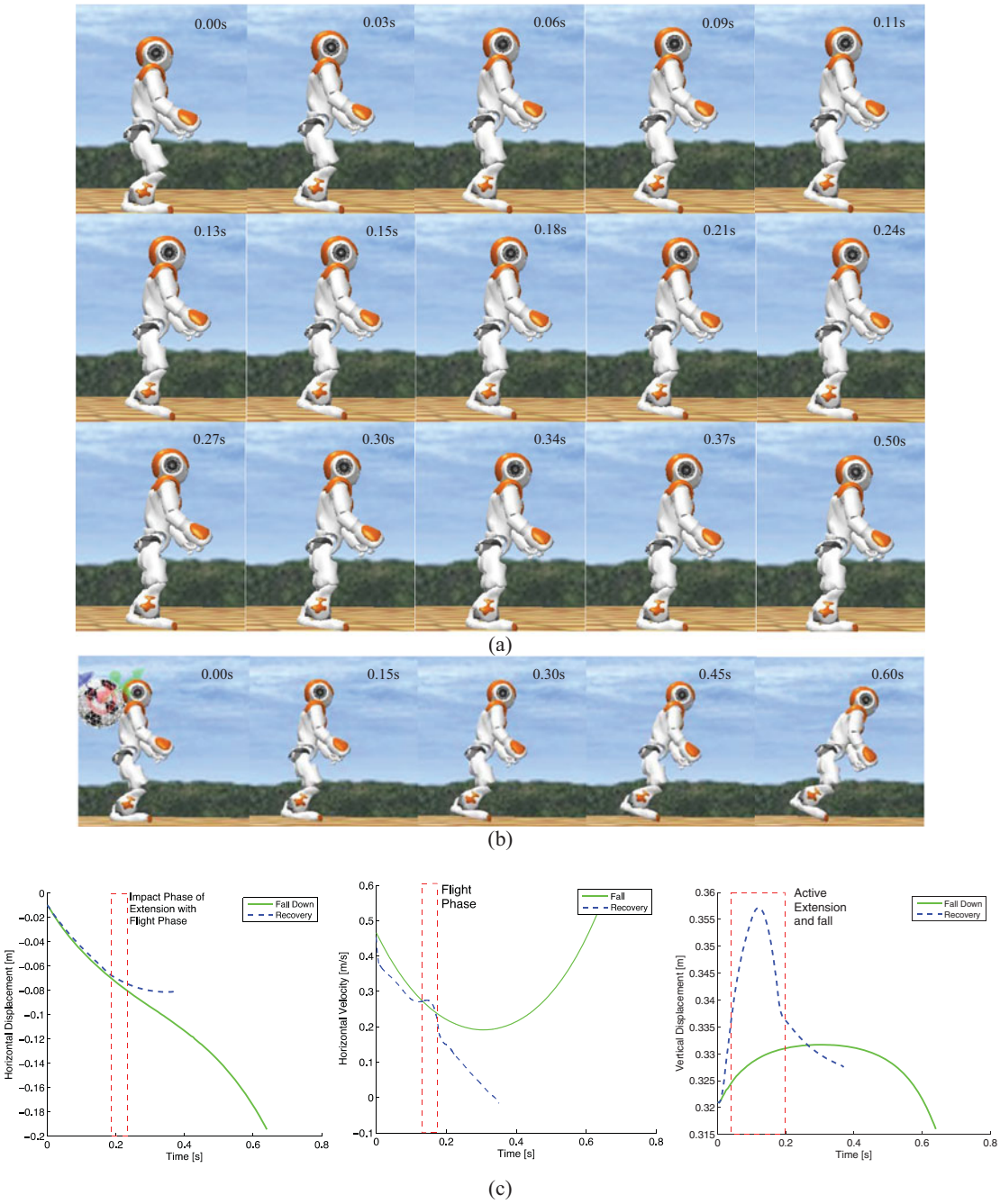


Fig. 12. (a) Image sequences showing that the robot recovers from a longitudinal push by using the extension strategy with flight phase in a double support state. (b) Image sequences showing that the robot eventually falls down without using the extension strategy when the same disturbance is applied. (c) The horizontal displacement, horizontal velocity and vertical displacement trajectories of the robot CoM.

Future work includes the development of an integral control system incorporated with our strategy on humanoid robots. Experimental investigations on the human body will also be conducted.

**Acknowledgements**

This work was supported in part by National Natural Science Foundation of China under Grant 51175288, 61375099 and 61533004, in part by Beijing Natural Science Foundation under Grant 3152014, and in part by Tsinghua University Initiative Scientific Research Program.

Downloaded from https://www.cambridge.org/core. Shaanxi Normal University, on 01 Jul 2020 at 19:14:54, subject to the Cambridge Core terms of use, available at https://www.cambridge.org/core/terms. https://doi.org/10.1017/S0263574716000308

**Supplementary material**

To view supplementary material for this article, please visit http://dx.doi.org/10.1017/S0263574716000308.

## References


1. M. Vukobratović and J. Stepanenko, "On the stability of anthropomorphic systems," *Math. Biosci.* **15**(1), 1–37 (1972).
2. S. Kajita and T. Kazuo, "Study of Dynamic Biped Locomotion on Rugged Terrain-Derivation and Application of the Linear Inverted Pendulum Mode," *IEEE International Conference on Robotics and Automation*, Sacramento, CA, USA (1991) pp. 1405–1411.
3. J. Pratt, J. Carff, S. Drakunov and A. Goswami, "Capture Point: A Step Toward Humanoid Push Recovery," *IEEE-RAS International Conference on Humanoid Robots*, Genoa, Italy (2006) pp. 200–207.
4. T. Koolen, T. De Boer, J. Rebula, A. Goswami and J. Pratt, "Capturability-based analysis and control of legged locomotion, Part 1: Theory and application to three simple gait models," *The Int. J. Robot. Res.* **31**(9), 1094–1113 (2012).
5. J. Pratt, T. Koolen, T. De Boer, J. Rebula, S. Cotton, J. Carff and P. Neuhaus, "Capturability-based analysis and control of legged locomotion, part 2: Application to m2v2, a lower body humanoid," *The Int. J. Robot. Res.* **31**(10), 1117–1133 (2012).
6. A. Hofmann and B. Williams, "Robust Execution of Temporally Flexible Plans for Bipedal Walking Devices," *The International Conference on Automated Planning and Scheduling*, Lake District, UK (2006) pp. 386–389.
7. Boston Dynamics. Available at: http://www.bostondynamics.com/, (2013).
8. X. Chen, Q. Huang, Z. Yu and Y. Lu, "Robust push recovery by whole-body dynamics control with extremal accelerations," *Robotica* **32**(3), 467–476 (2014).
9. C. Fu, "Perturbation Recovery of Biped Walking by Updating the Footstep," *IEEE/RSJ International Conference on Intelligent Robots and Systems*, Chicago, IL, USA (2014) pp. 2509–2514.
10. S. J. Yi, B. T. Zhang, D. Hong and D. D. Lee. "Online Learning of a Full Body Push Recovery Controller for Omnidirectional Walking," *IEEE-RAS International Conference on Humanoid Robots*, Bled, Slovenia (2011) pp. 1–6.
11. T. Li, P. Kuo, Y. Ho, M. Kao and L. Tai, "A biped gait learning algorithm for humanoid robots based on environmental impact assessed artificial bee colony," *IEEE Access*, **3**, 13–26 (2015).
12. V. B. Semwal, S. A. Katiyar, R. Chakraborty and G. C. Nandi, "Biologically-inspired push recovery capable bipedal locomotion modeling through hybrid automata," *Robot. Auton. Syst.* **70**, 181–190 (2015).
13. H. M. Maus, S. W. Lipfert, M. Gross, J. Rummel and A. Seyfarth, "Upright human gait did not provide a major mechanical challenge for our ancestors," *Nature Commun.* **1**, 70 (2010).
14. Aldebaran. Available at: https://www.aldebaran.com/ (2015).
15. Cyberbotics. Available at: http://www.cyberbotics.com/ (2015).
16. J. W. Fu, K. Chen, Z. Yu and Q. Huang, "A walking control strategy combining global sensory reflex and leg synchronization," *Robotica* **34**(5), 973–994 (2016).
17. C. Fu, F. Tan and K. Chen, "A simple walking strategy for biped walking based on an intermittent sinusoidal oscillator". *Robotica*, **28**(06), 869–884 (2010).
18. A. D. Kuo, "Energetics of actively powered locomotion using the simplest walking model," *J. Biomech. Eng.* **124**(1), 113–120 (2002).
19. C. Fu and K. Chen, "Gait synthesis and sensory control of stair climbing for a humanoid robot," *IEEE Trans. Ind. Electron.* **55**(5), 2111–2120 (2008).


## Appendix A: Approximation analysis

The approximations used in this paper are based on the following theorem in ordinary differential equations:

**Theorem:** Suppose that $f(t, x, \dot{x})$ and $g(t, x, \dot{x})$ are continuous on $(t, x, \dot{x}) \in \Omega$, $f(t, x, \dot{x}) < g(t, x, \dot{x})$ for $\forall (t, x, \dot{x}) \in \Omega$, and $f$ or $g$ is monotonically increasing with respect to $x$. Let $\phi_1(t)$ and $\phi_2(t)$ be the solutions to the following boundary value problem:

$$\ddot{x} = f(t, x, \dot{x}), \dot{x}(t_0) = \dot{x}_0, x(t_0) = x_0$$
$$\ddot{x} = g(t, x, \dot{x}), \dot{x}(t_0) = \dot{x}_0, x(t_0) = x_0.$$

Then for any $t > t_0$ and $(t, x, \dot{x}) \in \Omega$, we have

$$\phi_1(t) < \phi_2(t)$$
$$\dot{\phi}_1(t) < \dot{\phi}_2(t).$$

Downloaded from https://www.cambridge.org/core. Shaanxi Normal University, on 01 Jul 2020 at 19:14:54, subject to the Cambridge Core terms of use, available at https://www.cambridge.org/core/terms. https://doi.org/10.1017/S0263574716000308

*Proof:* Without loss of generality, let $t_0 = 0$. Define $\psi(t) = \phi_2(t) - \phi_1(t)$. We have

$$\psi(0) = 0$$
$$\dot{\psi}(0) = 0.$$

Under the continuous assumptions, $\exists\, \sigma > 0$, such that for $t \in (0, \sigma)$

$$\psi(t) > 0$$
$$\dot{\psi}(t) > 0.$$

Suppose that the conclusion $\phi_1(t) < \phi_2(t)$ is not true for $t > 0$, then there exists at least a $t_1$ such that $\psi(t_1) = 0$. Let

$$\beta = min\{t | \psi(t) = 0\}.$$

Then, $\psi(\beta) = 0$ and $\psi(t) > 0$ for $t \in (0, \beta)$. Therefore, $\dot{\psi}(\beta) \leq 0$, and there exists $0 < t_2 < \beta$ such that $\dot{\psi}(t_2) = 0$. Let

$$\alpha = min\{t | \dot{\psi}(t) = 0\}.$$

Then, $\dot{\psi}(\alpha) = 0$, and $\dot{\psi}(t) > 0$ for $t \in (0, \alpha)$. Hence, $\ddot{\psi}(\alpha) \leq 0$.
However,

$$\ddot{\psi}(\alpha) = g\left(\alpha, \phi_2(\alpha), \dot{\phi}_2(\alpha)\right) - f\left(\alpha, \phi_1(\alpha), \dot{\phi}_1(\alpha)\right) = g\left(\alpha, \phi_2(\alpha), \dot{\phi}_2(\alpha)\right) - f\left(\alpha, \phi_1(\alpha), \dot{\phi}_2(\alpha)\right) > g\left(\alpha, \phi_2(\alpha), \dot{\phi}_2(\alpha)\right) - f\left(\alpha, \phi_2(\alpha), \dot{\phi}_2(\alpha)\right) > 0$$

which is contradictory to the fact that $\ddot{\psi}(\alpha) \leq 0$. Thus $\phi_1(t) < \phi_2(t)$ is proved.
Suppose that the conclusion $\dot{\phi}_1(t) < \dot{\phi}_2(t)$ is not true for $t > 0$, then there exists at least a $t_3$ that $\dot{\psi}(t_3) = 0$. Let

$$\alpha = \min\{t | \dot{\psi}(t) = 0\}.$$

Then, $\dot{\psi}(\alpha) = 0$, and $\dot{\psi}(t) > 0$ for $t \in (0, \alpha)$. Hence,. However, by plugging $\phi_1(t) < \phi_2(t)$ and $f$ or $g$ is monotonically increasing with respect to $x$ ,

$$\ddot{\psi}(\alpha) = g\left(\alpha, \phi_2(\alpha), \dot{\phi}_2(\alpha)\right) - f\left(\alpha, \phi_1(\alpha), \dot{\phi}_1(\alpha)\right) = g\left(\alpha, \phi_2(\alpha), \dot{\phi}_2(\alpha)\right) - f\left(\alpha, \phi_1(\alpha), \dot{\phi}_2(\alpha)\right) > g\left(\alpha, \phi_2(\alpha), \dot{\phi}_2(\alpha)\right) - f\left(\alpha, \phi_2(\alpha), \dot{\phi}_2(\alpha)\right) > 0$$

which is contradictory to the fact that $\ddot{\psi}(\alpha) \leq 0$. Thus $\dot{\phi}_1(t) < \dot{\phi}_2(t)$ is proved.

Since the approximations used in this paper have similar governing equations, we would use (12) as an example, and the analysis steps on displacement and velocity of others are exactly the same as (12). The Eq. (12) could be written as

$$\ddot{x} = \frac{a_h}{z} x$$

where $z(t)$ is a time varying function and $0 < z(t) < z_0$, $a_h$ is a positive constant, $x < 0$ in the context. Let $f(t, x, \dot{x}) = \frac{a_h}{z} x$, $g(t, x, \dot{x}) = \frac{a_h}{z_0} x$. Set the initial conditions to be $\dot{x}(0) = \dot{x}_0$, $x(0) = x_0$ ,. We could see all the presuppositions are true. Thus, we concluded that

$$x(t) = \phi_1(t) < \phi_2(t)$$
$$\dot{x}(t) = \dot{\phi}_1(t) < \dot{\phi}_2(t)$$

Downloaded from https://www.cambridge.org/core. Shaanxi Normal University, on 01 Jul 2020 at 19:14:54, subject to the Cambridge Core terms of use, available at https://www.cambridge.org/core/terms. https://doi.org/10.1017/S0263574716000308

where $x(t)$,$\phi_2(t)$ are the solutions of

$$\ddot{x} = f\left(t, x, \dot{x}\right), \dot{x}\left(0\right) = \dot{x}_0, x\left(0\right) = x_0$$
$$\ddot{x} = g\left(t, x, \dot{x}\right), \dot{x}\left(0\right) = \dot{x}_0, x\left(0\right) = x_0.$$

Those expressions mean that the displacement and velocity calculated by our approximation $\phi_2(t) - x_0$ and $\dot{\phi}_2(t)$ are relatively larger than true value $x(t) - x_0$ and $\dot{x}(t)$. Thus, our estimated value, $\phi_2(t)$ and $\dot{\phi}_2(t)$, would predict a longer step according to the capture point dynamic for the capture point is proportional to horizontal velocity. Thus, we conclude that our approximation is conservative and lead to a longer capture distance.

## Appendix B: Electronic annexes

This paper has supplementary downloadable materials, as shown in Table I.

Table I. Electronic annexes.

| Annex | Type | Description | URL |
|---|---|---|---|
| 1 | Video | Forward recovery | http://learn.tsinghua.edu.cn:8080/2007990009/F.mp4 |
| 2 | Video | Lateral recovery | http://learn.tsinghua.edu.cn:8080/2007990009/L.mp4 |

Downloaded from https://www.cambridge.org/core. Shaanxi Normal University, on 01 Jul 2020 at 19:14:54, subject to the Cambridge Core terms of use, available at https://www.cambridge.org/core/terms. https://doi.org/10.1017/S0263574716000308